A Compact Ocean Bottom Electromagnetic Receiver and Seismometer

Kai Chen[1*], Ming Deng[1], Zhongliang Wu[2], Xianhu Luo[2], Li Zhou[1]

[1]School of Geophysics and Information Technology, China University of Geosciences (Beijing), Beijing, China

[2]MLR Key Laboratory of Marine Mineral Resources, Guangzhou Marine Geological Survey, Guangzhou, China

*Correspondence to: Kai Chen (ck@cugb.edu.cn).

Abstract. Joint marine electromagnetic (EM) and seismic interpretation are widely used for offshore gas hydrate and petroleum exploration, to produce improved estimates of lithology and fluids, and decrease the risk of low gas saturation. However, joint data acquisition is not commonly employed. Current marine EM data acquisition depends on an ocean bottom electromagnetic receiver (OBEM) and current seismic exploration methods use seismometers. Joint simultaneous data acquisition can decrease costs and improve efficiency but conventional independent data receivers have several drawbacks, including a large size, high costs, position errors, and low operational efficiencies. To address these limitations, we developed a compact ocean bottom electromagnetic receiver and seismometer (OBEMS). Based on existing ocean bottom E-field receiver (OBE) specifications, including low noise levels, low power consumption, and low clock-drift errors, we integrated two induction coils for the magnetic sensor and a three-axis omni-directional geophone for the seismic sensor to assemble an ultra-short base line (USBL) transponder as the position sensor, which improved position accuracy and operational efficiency while reducing field data acquisition costs. The resulting OBEMS has a noise level of 0.1 nV/m/rt (Hz) at 1 Hz in the E-field, 0.1 pT/rt (Hz) at 1 Hz in the B-field, and a 30-day battery lifetime. This device also supports a WiFi interface for the configuration of data acquisition parameters and data download. Offshore acquisition was performed to evaluate the system's field performance during offshore gas hydrate exploration. The OBEMS operated effectively throughout the operation and field testing. Therefore, the OBEMS can function as a low cost, compact, and highly efficient joint data acquisition method.

1. Introduction

Marine electromagnetic (EM) and seismic methods are important geophysical tools used for offshore petroleum exploration (Barsukov and Fainberg, 2017; Constable and Srnka, 2007; Ellingsrud et al., 2002), gas hydrate mapping (Schwalenberg et al., 2017; Weitemeyer et al., 2006), physical oceanography (Zhang et al., 2014), crustal studies (Constable and Heinson, 2004; Key and Constable, 2002; Kodaira et al., 2000), mid-ocean ridge studies (Key, 2012), subduction zone studies (Naif et al., 2015), and underwater target detection (ISL, 2016). To improve the interpretation accuracy and decrease the risks associated with offshore drilling, surveys increasingly conduct multi-physics integrated interpretation and cooperative inversion, such as joint marine EM and seismic interpretations (Goswami et al., 2015; Goswami et al., 2017; Weitemeyer et al., 2011). In offshore exploration, seismic and EM data acquisition are typically performed independently. Joint offshore seismic and EM data acquisition would not only increase the efficiency and decrease costs, but also improve the interpretation

accuracy (Engelmark et al., 2012). Complementary data also enhance our understanding of subsurface characteristics. While seismic methods provide an indication of the subsurface architecture, EM is more sensitive to changes in fluids. Seismic data can be inverted for velocity and acoustic impedance while EM data inversion provides resistivity values. Correlating these two methods has the potential to improve hydrocarbon saturation estimates and drilling success rates.

Ocean bottom electromagnetic receivers (OBEM) are used to measure seafloor magnetotelluric (MT) and controlled source electromagnetic (CSEM) field signals. Jean Filloux and colleagues performed the first seafloor EM measurements made using the MT method in the 1960s (Filloux, 1967). More recently, the Scripps Institution of Oceanography (SIO) collaborated with Quasar to design a small EM receiver (QUASAR, 2019) based on the existing SIO EM receiver (Constable, 2013) for compact and low cost EM data acquisition. The resulting QMax EM3 receiver optimized the efficiency and safety, enabling survey contractors to achieve faster deployment and recovery times, use more receivers, and perform more surveys in a shorter time period (QUASAR, 2019). Kasaya (2009) also developed a small OBEM and ocean bottom electrometer (OBE) system that had an arm-folding mechanism to facilitate assembly and recovery operations. For magnetic observations, they used a fluxgate sensor. This OBE mainly focuses on marine MT acquisition and the CSEM is not included. Current trends in instrumentation involve smaller sizes, lower power consumptions, lower noise levels, and lower data acquisition costs. Marine EM field data acquisition technology continues to improve with reduced costs and increased flexibility.

Ocean bottom seismometers (OBS) have been employed to produce offshore seismographs since the 1970s. OBS are usually equipped with three component geophones to record sound waves generated by either earthquakes at depth or man-made devices near the surface. They record the movement of the seafloor in all directions while a hydrophone records the pressure in the surrounding water. The French Research Institute for Exploitation of the Sea (IFREMER) (Auffret et al., 2004) developed a new generation of ocean bottom seismometers by integrating acquisition and instrument release, adding a rechargeable battery, enabling data downloads via USB cable, and reducing the unit's size. GeoPro GmbH developed a similar system whose CPU and recorder are housed in a 17-inch glass sphere. Panahi et al. (2008) designed a low power data logger for OBS systems based on a compact flash card. Sercel and Geopro are currently the leading manufacturers in the OBS market. All their instruments are designed for low power consumptions, low noise levels, low time drift errors, and a compact size.

Marine controlled-source electromagnetic (CSEM) sounding is a new tool available to geophysicists for offshore gas hydrate exploration (Weitemeyer, 2011). This technique has been developed to detect deep hydrocarbon reservoirs (Fanavoll, 2010). The OBEM is the receiver that measures the EM field for the marine CSEM and/or MT method. The OBS mainly provides deep geological information and is also used for shallow gas hydrate mapping (Mienert, 2005). Therefore, these two offshore active/passive geophysical exploration instruments can jointly provide a complementary image to identify natural resources and/or geologic structures. Thus, combining OBEM and OBS data acquisition to investigate gas hydrate or petroleum exploration within a few kilometers below the seafloor is desirable.

Current offshore EM and seismic data acquisition typically employ both OBEM and OBS, but the two instruments operate independently. There are two disadvantages to independent data acquisition: 1) the error related to each individual instrument position and 2) the cost of offshore data acquisition, which includes

instrument hardware, research vessels, and human resources, among other factors. Considering the former, the quality of marine CSEM data is dependent on accurate navigational information for both the transmitter and receiver positions and orientations. Current OBEMs locate via acoustic release, such that it has a greater position error and uses the near field to refine the geometry of the transmitter and receiver locations (Weitemeyer, 2011), which are dependent on data post-processing. Position errors may lead to reduced inversion accuracy.

Both KMS and GeoSYN have developed a GEOSYN/KMS 870-VectorSeisEM Broadband-Ocean bottom station, which is a broadband 4C seismic/6C electromagnetic node for shallow and deep water geophysical applications. Using a single survey vessel, Petroleum Geo-Services Inc. (PGS) can acquire high-density EM data simultaneously with 2-D GeoStreamer® seismic data or high-density 3-D EM data over existing or planned 3-D seismic data. Offshore high-density joint EM and seismic acquisition and integrated data analysis represents a stepwise change in the application of EM technology. Both technologies seek to mitigate risk when searching for and extracting oil and gas. During 2010, we acquired coincident marine CSEM and OBS data when PGS conducted one of the first field trials of their towed streamer EM system at the Troll field, located in the Norwegian North Sea (Zhdanov et al. 2012). The towed streamer EM system allowed the acquisition of CSEM data simultaneously with seismic data over large areas, resulting in higher production rates and lower costs than those associated with conventional CSEM acquisition.

The China University of Geosciences (Beijing) (CUGB) developed an OBEM in 1998 (Deng et al., 2003). During the past 20 years, CUGB has successfully used its OBEM equipment in deep EM surveys for gas hydrate mapping and hydrocarbon exploration (Wei et al., 2009; Jing et al., 2016). The OBEM has also been widely used for marine magnetotelluric and CSEM measurements. The current OBEM system has an acoustic telemetry modem and a folding-arm mechanism (Chen et al., 2015), with low noise levels and low time drift errors. In 2014, CUGB developed a micro OBE for low cost and highly efficient data acquisition (Chen et al., 2017). To achieve joint EM and seismic data acquisition, the instrument was upgraded from an existing micro OBE by 1) integrating a three-axis omni-directional geophone for seismic parameter measurements, 2) installing two induction coils for horizontal magnetic field component measurements, and 3) installing an ultra-short baseline (USBL) transponder for tracking the seafloor position as the system ascends after release.

The ocean bottom electromagnetic receiver and seismometer (OBEMS) has been mechanically optimized to satisfy all technical requirements for simultaneous joint seismic and electromagnetic data acquisition. This technical advancement permits enhanced modeling and the simultaneous interpretation of both datasets, which minimizes acquisition costs. The advantages of this OBEMS include 1) lower cost and higher efficiency of both the instrument and offshore data acquisition, as the same cost includes more nodes required to improve the horizontal resolution and 2) a smaller seafloor instrument position error, which decreases the inversion error. The OBEMS system can also replace an OBEM as the receiver in marine CSEM surveys. In addition, the OBEMS can be used for OBS observations. In the future, a hydrophone will be added to the OBEMS system to allow measurements of the acoustic pressure field.

2. Instrument specifications

To achieve joint EM and seismic data acquisition with the objectives of reducing the data acquisition cost and improving operational efficiency, we developed a new OBEMS. The OBEMS was then used to record the seafloor EM field and acoustic signals. Figure 1 shows a schematic of the system. The OBEMS consists of a nylon frame, two glass spheres, a red flag, a transducer, a USBL transponder, a data logger, a battery, three geophones, four electrodes, two induction coils, and an anchor. The equipment is fixed onto a nylon frame measuring 105 cm × 55 cm × 65 cm. All electronics are installed inside a 17-inch glass sphere, except for the transducer and USBL, while the other glass sphere provides buoyancy. Figure 2 shows a photo of the OBEMS while floating to the surface. We used Ag/AgCl electrodes to measure the electric voltage in the Ex and Ey dipoles. The E-field noise level was 0.1 nV/m/rt (Hz) at 1 Hz (at a working water depth of 1,000 m), with a 12 m dipole. We used commercial omni-directional geophones (ODG8 geophone, manufactured by Chongqing Geological Instrument Factory) as seismometers, with an 8 Hz natural frequency, to record three artificial orthogonal earthquake signal components. Omnidirectional geophones were used because traditional geophones cannot effectively and reliably receive vibration signals on an inclined seabed. In addition, an AHRS was installed to measure the orientation and inclination of the geophone for further data processing. The moving coil geophone may generate EM noise on the magnetic sensors, but the electronics (data acquisition circuit board, battery, and geophone) are all shielded by ferrite film and the distance between the induction coil and geophone is too large to measure the EM noise. We confirmed the EM noise of the geophone by testing it in a magnetically shielded room. The geophone sensitivity was 78.5 V/m/s at 15 Hz and the internal resistance was 3,100 Ω. Four sets of six 18,650 Li-ion rechargeable batteries (for 25.2 V) supply power to the data logger circuit. One independent 16.8 V battery supplies power to the acoustic telemetry modem (ATM) module. The power consumption is approximately 1 W at a maximum sampling rate of 2,400 Hz and the power supply module supports data acquisition for ~30 days.

The OBEMS data logger has a 24 bit analog-to-digital converter for each of the two electrical field components and the three-axis geophone components. The attitude and heading reference system (AHRS) module records the pitch, roll, and heading while the instrument is on the seafloor. The OBEMS has two parallel release mechanisms. The transducer connects with the ATM for acoustic telemetry. When the ATM receives the release command, the burn-wire mechanism release is driven and the anchor releases after 10 minutes. Additionally, a USBL transponder responder and motor-driven release were installed on the OBEMS. The transponder is designed for positioning remotely operated vehicles (ROVs), towed fish, and other mobile targets in water depths up to 4,000 m and is equipped with an omni-directional transducer for a wide range of general USBL tracking applications. The transponder is available with acoustically controlled output lines suitable for an external motor drive. This transponder integrated the USBL transponder, release, and an internal depth sensor to improve USBL position performance.

The resulting reduction in the positioning uncertainty leads to significant improvements in the target sensitivity. Acoustic ultra-short baseline communication (USBL) is used to establish the exact receiver positions. The OBEMS integrated a USBL transponder from Sonardyne (GyroUSBL) to determine the underwater acoustic positioning, whose accuracy is approximately 1.5‰ of the slant distance. When the slant distance is 2,000 m, we estimate that the receiver positions obtained in this manner are accurate to

To maintain a simple and compact OBEMS design, the seismometers were indirectly coupled to the seafloor via the sphere, release hardware, anchor, and spring used to connect the OBS to the anchor. While seismometers work best when they are in direct contact with the Earth (Mànuel et al., 2012), this design has been proven effective for collecting data at long shot-receiver offsets. Coupling the instrument to the seafloor is important, as the geophone, which measures seafloor movement, is located inside the sphere rather than deployed on the seafloor. To further optimize coupling, a weight in the shape of a cross with a U-shaped strap was used to ensure good penetration of the anchor weight into the seafloor. The single U-shaped stainless steel strap connects the two burn-wire mechanisms, passing through two stainless steel loops set into the anchors.

To provide the highest possible accuracy, time was recorded to the nearest millisecond. Each OBEMS uses a microprocessor controlled crystal oscillator (MCXO) as a stable clock reference, for which the drift can be as little as 2 ms/day. Following each deployment, the offset was measured to compensate for the total time drift. The size of the anchor is 110 cm x 60 cm x 6 cm, weighing 136 kg in air and 78 kg in water. During deployment, the weight of the OBEMS in water is 42 kg and –36 kg upon ascent. The redundant buoyancy is designed for the addition of more batteries for a longer seafloor working time. The descent and ascent velocities of the OBEMS are approximately 1 and 0.8 m/s, respectively. Table 1 lists the specifications of the OBEMS system.

3. Electronics

Figure 3 shows a schematic of the OBEMS data logger. The data logger is based on a 24-bit analog-to-digital converter (ADC) for each channel. Different analog pre-amplifiers were used for the electric field, magnetic field, and geophone measurements. The data logger contains eight channels. Each channel integrates a pre-amplifier and a 24-bit ADC. The pre-amplifier for the E-field channel is an ultra-low noise chopper amplifier that has been upgraded from Constable (2013). The self-noise level is approximately 0.6 nV/rt(Hz) at 1 Hz, the gain is 1,200, and the –3 dB bandwidth is 0.01 Hz to 100 Hz. The pre-amplifier for the geophone is a different amplifier with a gain of 20 dB. The gain of the induction coil is 300 mV/nT and the output range is ± 5 V. The input range of the ADC is ± 5 Vpp to match the pre-amplifier and ranges of the induction coil output. The ADC module is based on an eight-channel, 24-bit ADC, i.e., the ADS1282 (TI). The ADS1282 is a one-channel, high dynamic range, fourth order Δ-Σ modulator, with a digital filter for data decimation and interfacing with the microcontroller module, which provides a dynamic range of 130 dB at a 250 Hz sampling rate and a total harmonic distortion (THD) of –122 dB. The full scale of the ADC is ± 2 V, with an attenuation coefficient of 0.4.

A Micro-control unit (MCU) A (AT91SAM9G45 from ATMEL) is the master MCU, which is used to set the sampling rate, configure the ADC register; write data to the SD card; communicate with a computer via a WiFi module; and communicate with the slave MCU B (ATmega16 from ATMEL), the attitude and heading reference system (AHRS) module, and the GPS module via a serial port. The complex programmable logic

device (CPLD) (EPM570 from INTEL) reads, in parallel, converted data from the eight ADCs and series data awaiting MCU A data transfer. The MCU A employs an internal direct memory access (DMA) controller and writes data to the SD card. The MCXO (MX-503 from Vectron) has a low power consumption of 3.3 V and 12 mA, with a high-frequency stability of approximately ± 20 ppb from 0 to 50°C. The CPLD generates a 2.4576 MHz clock as the ADC master clock. The selectable sampling rate can be set to 2,400, 600, or 150 Hz, with a dynamic range that reaches approximately 115, 121, and 127 dB, respectively.

MCU B is used as the slave MCU for communication with the ATM, driving the burn wire current source, measuring battery capacity, and as a pressure sensor inside the glass sphere for negative pressure monitoring to determine if there is a leak in the glass sphere. When the ATM receives the release command, MCU B drives the current source and provides 500 mA to the burn-wire release. A charger module converts the external DC 28 V to independently charge each Li-ion rechargeable battery pack.

The collected data are stored on an SD card. To download the data, there is no need to open the glass sphere or use an Ethernet wire. A computer can connect to the data logger to download the data and configure acquisition parameters using the onboard WiFi module. The capacity of the SD card is 32 GB, which can be expanded to 128 GB. The sampling rate was set to 150 Hz, generating 400 MB of data per day. An effective download speed of 3 MB/s was achieved, which allows 30 days of data (approximately 12 GB) to be downloaded in less than 67 min. After the OBEMS is released from its anchor, floating at the surface, it can be recovered using radio signals detected by a 165 MHz Very High Frequency (VHF) direction finder at distances of up to 5 km, even in poor visibility. The flashing light inside the sphere is especially useful for recovery at night. Figure 4 shows a photo of the data logger installed in the glass sphere.

4. Offshore experiments

In August 2018, we conducted offshore experiments to map gas hydrates in the Qiongdongnan region of the South China Sea. The support vessel used was the *Hai Yang Si Hao*, which is registered with the Guangzhou Marine Geological Survey Bureau. This expedition was the result of a collaboration between the Guangzhou Marine Geological Survey and CUGB. The scientific objective of the cruise was to map gas hydrates using a marine EM method while also using CSEM to determine the electrical structure 500 m below the seafloor. To achieve this, 20 previously developed OBEMs and a towed CSEM transmitter (Wang et al., 2017) were operated during the cruise. To evaluate the overall performance of the receiver described in this study, two OBEMS were also used.

The Qiongdongnan region of the South China Sea is located 170 km southeast of Sanya. The seafloor is an ocean basin with depths of 1,700–1,800 m. Figure 5 shows a map of the experimental area, which included 22 receivers. Here, R19 and R21 indicate the two newly developed OBEMS while other labels represent the other existing OBEMs. All receivers were equipped with USBL transponders. When the receiver began its descent to the seafloor, the transponder tracked its position. If the depth of the receiver did not change substantially, the location result was assumed to indicate its landing position. After all receivers were deployed, two transmitter lines were towed for different waveforms: a single square waveform at 8 Hz and multiple frequencies synthesized with a 0.5 Hz fundamental frequency. After 10 days on the seafloor, all 20 OBEMs and the two OBEMS units were successfully recovered.

We estimated the MT responses (apparent resistivities and phase differences) using the robust estimate method (Egbert, 1997). To calculate the MT responses at site R19, Fig. 6 shows the respective computed MT responses for the site over a period of 10 to 10,000 s. The data quality was excellent down to periods of approximately 10,000 s. At high frequencies, we observed the sea floor response for both modes asymptotic to 1 Ωm.

The CSEM data acquisition employed a towed CSEM transmitter with a length of 300 m that generated horizontal electrical dipoles (HED) while the altimeter of the towed transmitter body was approximately 20–50 m. The transmitters were used at a single frequency of 8 Hz and multiple frequencies synthesized with a fundamental frequency of 0.5 Hz. The transmitter was equipped with a depth sensor, altimeter, and acoustic transponder. The transmitter transmitted at 450 A. The OBEMS received CSEM data, followed by the performance of the horizontal E-field and B-field component Fast Fourier Transforms (FFT), current data FFT, instrument calibration, and field component rotation. Figure 7 shows the Ex component of site R19's signal spectrum. The result of the short time Fourier transform (STFT) clearly shows the two towed CSEM lines (i.e., the 8 and 0.5 Hz towed lines). Figure 8 shows the MVO of the horizontal EM component at site R19. The 8 Hz data are above the instrumental noise floor at a 3.5 km range.

After CSEM data acquisition using a towed transmitter source, seismic data acquisitions were performed by testing the functionality of the OBEMS using an air gun as the source. Figure 9 shows the single shot waveforms. The vertical peaks in each channel correspond to the acquisition of the reflected and refracted acoustic signals generated by the artificial source. The recordings show clear vibration signal arrivals, which demonstrate the proper functioning of all three geophone channels. Figure 10 shows the power spectra of the three components estimated using the 200 s time series and the ground noise power spectra. The main air gun energy was focused at 40–60 Hz. Due to the low sampling rate (150 Hz), higher frequency band signals are depressed.

5. Conclusions

To achieve joint marine EM and seismic data acquisition, we developed an OBEMS based on an existing micro-OBE receiver, which consisted of two induction coils for horizontal magnetic field component measurements and a three-axis omni-directional geophone for recording seafloor movement in all directions, as well as an assembled a USBL transponder for seafloor position tracking. The final system included four electrodes, three geophones, two induction coils, two glass spheres, USBL transponder, motor drive release, integrated ATM, burn-wire release mechanism, recovery beacon (LED, radio modem, and VHF radio), and an expanded Wi-Fi module for data transfer. A 17-inch glass sphere contains the data logger and battery. The proposed OBEMS architecture exhibited low noise, low clock drift, and low-power specifications. The OBEMS was mechanically optimized to satisfy all technical requirements for the simultaneous acquisition of seismic and electromagnetic data. However, the following minor technical improvements will be made in future studies:

1) The autonomy of the instrument will be extended to 60 days of data acquisition and 90 days on the seafloor.

2) A hydrophone will be installed to achieve a fully integrated all-in-one receiver.

3) Enhancements to WiFi module performance.

As these preliminary tests have shown, OBEMS technology is capable of high quality MT, CSEM, and artificial seismic data acquisition. Future developments to this instrument will add a hydrophone and lengthen the seafloor working time (2-3 months), which add to the existing advantages of the OBEMS (i.e., low cost, easy deployment, small size, and high efficiency). These developments will occur through a cooperation between the GMGS and CUGB.

Data availability

The raw data from the experiments are available upon request (ck@cugb.edu.cn).

Author contributions

K.C. designed the new instrument and wrote the manuscript. M.D. was the project leader. Z.L.W. and X.H.L. provided ideas and guidance, including on the experiment. L.Z. designed and tested the electronics.

Competing interests

The authors declare that they have no conflicts of interest.

Acknowledgments

The development of the OBEMS was supported by the National High Technology Research and Development Program of China (Nos. 2016YFC0303100 and 2017YFF0105700) and the Key project of the National Science Foundation of China (Nos. 61531001 and 41804071). The development of the low-noise electrode and amplifier was supported by the Fundamental Research Funds for the Central Universities (Nos. 2652015403 and 2652018265). Joint data acquisition was partially supported by the China Geological Survey (No. GZH-201100307). We also acknowledge the extensive support offered by the captain, ship's crew, and marine technicians of the R/V *Hai Yang Si Hao*, as well as Dr. Jing for EM data processing, Professor Zhao for technical help, and Dr. Tu for helpful comments and support. The instruments were carefully manufactured and modified by Professor Zhang.

References

Auffret, Y., Pelleau, P., Klingelhoefer, F., Geli, L., Crozon, J., Lin, J. Y., Sibuet J. : MicrOBS: A new generation of ocean bottom seismometer, *First break,* 22(7), 4–147, 2004.

Barsukov, P. O. and Fainberg, E. B.: Marine transient electromagnetic sounding of deep buried hydrocarbon reservoirs: principles, methodologies and limitations, *Geophysical Prospecting,* 65(3), 840–858, 2017.

Chen, K., Deng, M., Luo, X., and Wu, Z.: A micro ocean-bottom E-field receiver, *Geophysics,* 82(5), E233–E241, 2017.

Chen, K., Wei, W., Deng, M., Wu, Z., and Yu, G.: A new marine controlled-source electromagnetic receiver

295   with an acoustic telemetry modem and arm-folding mechanism, *Geophysical Prospecting,* 63(6), 1420–1429, doi:10.1111/1365-2478.12297, 2015.

Constable, S. and Heinson, G.: Hawaiian hot-spot swell structure from seafloor MT sounding, *Tectonophysics,* 389(1-2), 111–124, 2004.

Constable, S. C.: Review paper: Instrumentation for marine magnetotelluric and controlled source

300   electromagnetic sounding, *Geophysical Prospecting,* 61, 505–532, 2013.

Constable, S. C. and Srnka, L. J.: An introduction to marine controlled-source electromagnetic methods for hydrocarbon exploration, *Geophysics,* 72(2), WA3–WA12, 2007.

Deng, M., Wei, W., and Handong, T.: Collector for seafloor magnetotelltic data, *Chinese Journal of Geophysics,* 2, 217–223, 2003.

305   Ellingsrud, S., Eidesmo, T., Johansen, S., Sinha, M., MacGregor, L., and Constable, S.: Remote sensing of hydrocarbon layers by seabed logging (SBL): Results from a cruise offshore Angola, *The Leading Edge,* 21(10), 972–982, 2002.

Engelmark, F., Mattsson, J., and Linfoot, J.: Simultaneous acquisition of towed EM and 2D seismic? A successful field test, *ASEG Extended Abstracts,* 2012(1), 1–4, 2012.

310   Fanavoll S, Hesthammer J, Danielsen J, Stefatos, A.: Controlled source electromagnetic technology and hydrocarbon exploration efficiency, *First Break*, 28(5), 2010.

Filloux, J. H.: An ocean bottom, D component magnetometer, *Geophysics,* 32(6), 978, 1967.

Egbert, G. D.: Robust multiple-station magnetotelluric data processing, *Geophys. J. Int.,* 130, 475– 496, 1997.

Goswami, B. K., Weitemeyer, K. A., Bünz, S., Minshull, T. A., Westbrook, G. K., Ker, S., and Sinha, M. C.:

315   Variations in pockmark composition at the Vestnesa Ridge: Insights from marine controlled source electromagnetic and seismic data, *Geochemistry, Geophysics, Geosystems,* 18(3), 1111–1125, 2017.

Goswami, B. K., Weitemeyer, K. A., Minshull, T. A., Sinha, M. C., Westbrook, G. K., Chabert, A., Henstock, T. J., and Ker, S.: A joint electromagnetic and seismic study of an active pockmark within the hydrate stability field at the Vestnesa Ridge, West Svalbard margin, *Journal of Geophysical Research: Solid Earth,* 120(10),

320   6797–6822, 2015.

ISL.: http://www.islinc.com/solutions/advanced-sensor-technologies/. Last access: 1 June 2019, 2016.

Jing J.-E., Wu, Z. L., Deng, M., Zhao, Q. X., Luo, X. H., Tu, G. H., Chen, K., Wang, M.: Experiment of marine controlled-source electromagnetic detection in a gas hydrate prospective region of the South China Sea, *Chinese Journal of Geophysics,* 59(7), 2564–2572, 2016.

325   Mienert, J., Bünz, S., Guidard, S., Vanneste, M., Berndt, C.: Ocean bottom seismometer investigations in the Ormen Lange area offshore mid-Norway provide evidence for shallow gas layers in subsurface sediments, *Marine and Petroleum Geology*, 22, 287–297, 2005.

Kasaya, T. G., T.-N.: A small ocean bottom electromagnetometer and ocean bottom electrometer system with an arm-folding mechanism (Technical Report), *Exploration Geophysics,* 40(1), 41–48, 2009.

330   Key, K.: Marine Electromagnetic Studies of Seafloor Resources and Tectonics, *Surveys in Geophysics,* 33(1), 135–167, 2012.

Key, K. and Constable, S.: Broadband marine MT exploration of the East Pacific Rise at 9°50 ' N, *Geophysical Research Letters,* 29(22), 2002.

Kodaira, S., Takahashi, N., Park, J.-O., Mochizuki, K., Shinohara, M., and Kimura, S.: Western Nankai Trough seismogenic zone: Results from a wide-angle ocean bottom seismic survey, *Journal of Geophysical Research,* 105(B3), 5887–5905, 2000.

Mànuel, A., Roset, X., Rio, J. D., Toma, D. M., Carreras, N., Panahi, S. S., Benad, A. G., Owen, T., Cadena, J.: Ocean Bottom Seismometer: Design and Test of a Measurement System for Marine Seismology, *Sensors,* 12(3), 3693–3719, 2012.

Naif, S., Key, K., Constable, S., and Evans, R. L.: Water-rich bending faults at the Middle America Trench, *Geochemistry, Geophysics, Geosystems,* 16(8), 2582–2597, 2015.

Panahi, S. S., Ventosa, S., and Cadena, J.: A Low-Power Datalogger Based on CompactFlash Memory for Ocean Bottom Seismometers, *IEEE Transactions on Instrumentation & Measurement,* 57(10), 2297–2303, 2008.

QUASAR – GEOPHYSICALTECHNOLOGIES. http://www.quasargeo.com/qmax.html. last access: 1 June 2019, 2019.

Schwalenberg, K., Rippe, D., Koch, S., and Scholl, C.: Marine-controlled source electromagnetic study of methane seeps and gas hydrates at Opouawe Bank, Hikurangi Margin, New Zealand, *Journal of Geophysical Research: Solid Earth,* 122(5), 3334–3350, 2017.

Wang, M., Deng, M., Wu, Z., Luo, X., Jing, J., and Chen, K. :The deep-tow marine controlled-source electromagnetic transmitter system for gas hydrate exploration, *Journal of Applied Geophysics,* 137, 138–144, 2017.

Wei, W., Deng, M., and Wen, Z.: Experimental Study of Marine Magnetotelluric in Southern Huanghai, *Chinese Journal of Geophysics,* 52(2), 440–450, 2009.

Weitemeyer, K. A., Constable, S., and Tréhu, A. M.: A marine electromagnetic survey to detect gas hydrate at Hydrate Ridge, Oregon, *Geophysical Journal International,* 187(1), 45–62, 2011.

Weitemeyer, K. A., Constable, S. C., Key, K. W., and Behrens, J. P.: First results from a marine controlled-source electromagnetic survey to detect gas hydrates offshore Oregon, *Geophysical Research Letters,* 33(3), L03304, 2006.

Zhang, L., Baba, K., Liang, P., Shimizu, H., and Utada, H.: The 2011 Tohoku Tsunami observed by an array of ocean bottom electromagnetometers, *Geophysical Research Letters,* 41(14), 4937–4944, 2014.

Zhdanov, M. S., Endo, M., Čuma, M., Linfoot, J., Cox, L. H., and Wilson, G. A.: The first practical 3D inversion of towed streamer EM data from the Troll field trial, In *Seg Technical Program Expanded,* 2012, 1-5, 2012.
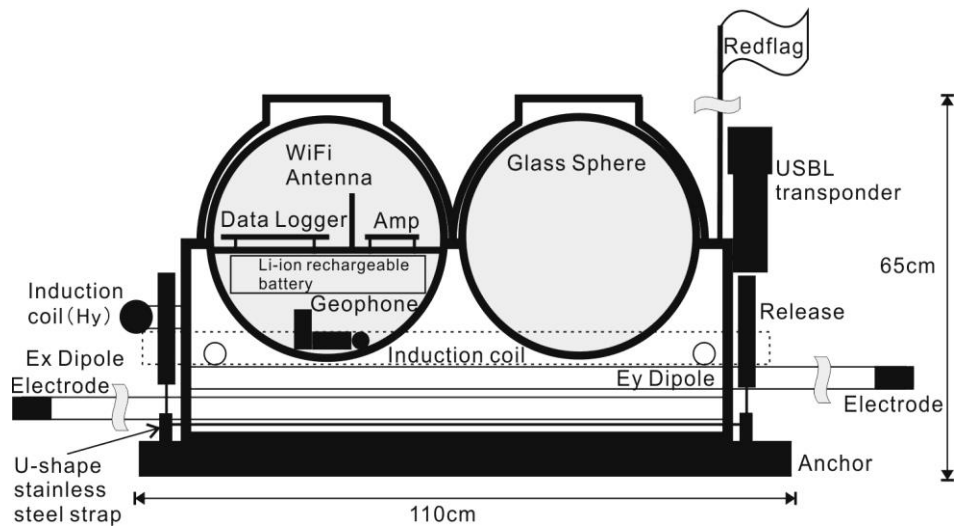
Fig. 1. Schematic diagram of the ocean bottom electromagnetic receiver and seismometer (OBEMS). Diagram shows the structural design inside the glass sphere, with omni-directional geophones in the lowest layer, followed by the Li-ion rechargeable battery packs, Acoustic Telemetry Modem (ATM), and the data logger. All print circuit boards are covered with magnetic shielding. Ferrite sheets, with a 0.01-mm-thick film on one side and a 0.02-mm-thick adhesive tape on the other, were glued inside the shielding box. These ferrite sheets function primarily as suppressors, blocking EM noise at lower frequencies and absorbing it at higher frequencies. A single U-shaped stainless steel strap connects the two release mechanisms, passing through two stainless steel loops set into the anchors.

370

375
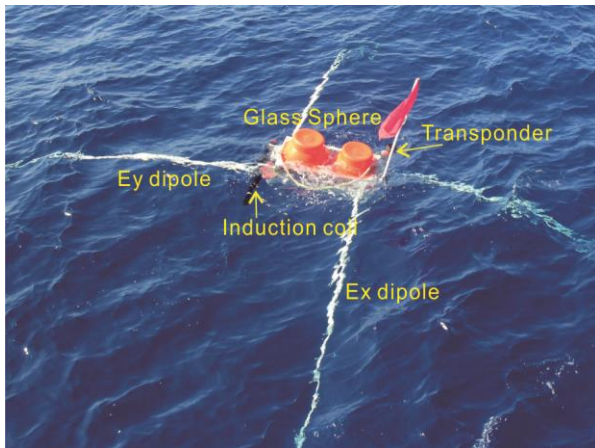
Fig. 2. Photograph of the OBEMS while in the water ascending to the surface after release. The length of the electrode dipole is 12 m.

380
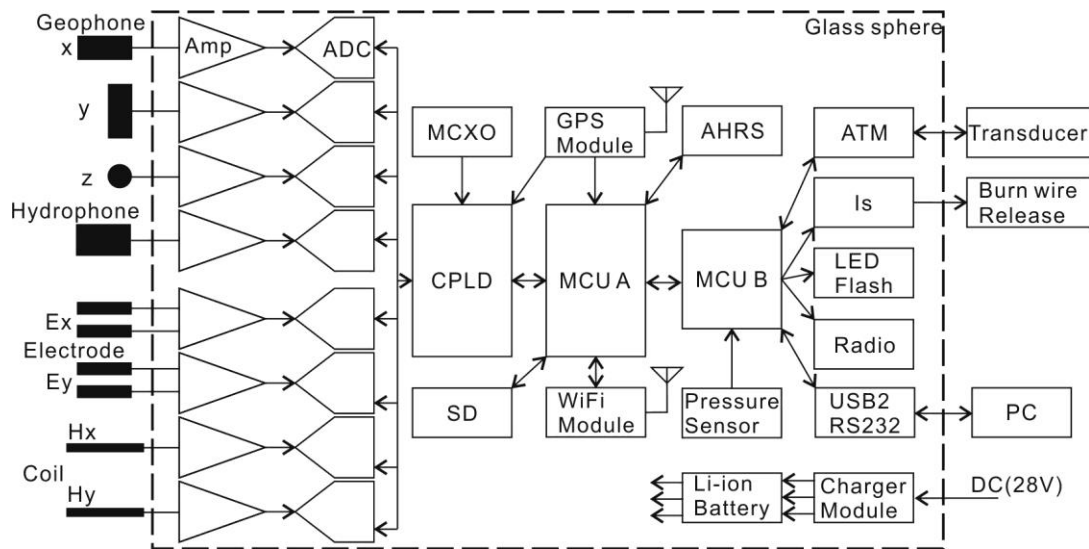
Fig. 3. Circuit diagram of the OBEMS data logger, containing EM and seismic sensors, eight amplifiers, eight analog to digital converters (ADC), a complex programmable logic device (CPLD), secure digital memory card (SD), microprocessor controlled crystal oscillator (MCXO), Li-ion rechargeable battery, charger module, LED Flash, Radio, ATM, and attitude heading reference system (AHRS). In this preliminary design, the ATM, burn wire release, ultra-short base line (USBL), and relay release are all designed for release.
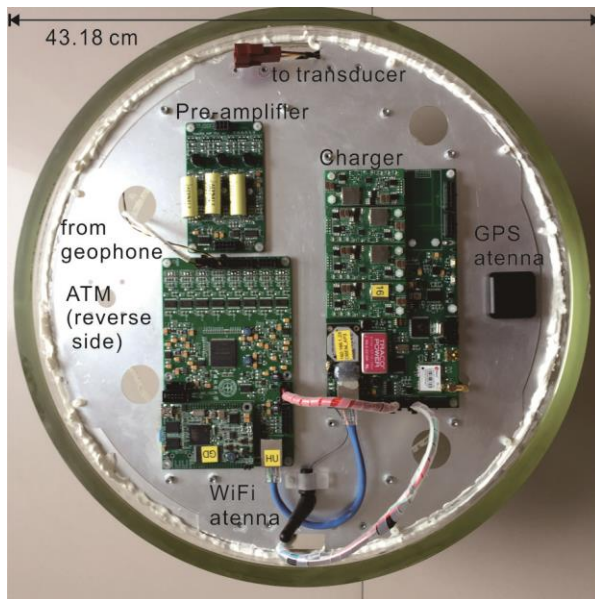
385

Fig. 4. Photo of the data logger installed in the glass sphere. Under the aluminum board, an ATM, Li-ion rechargeable battery set, and three-axis geophone are fixed. After circuit assembly, magnetic shielding covers the three print circuit boards to decrease sensor disturbance.
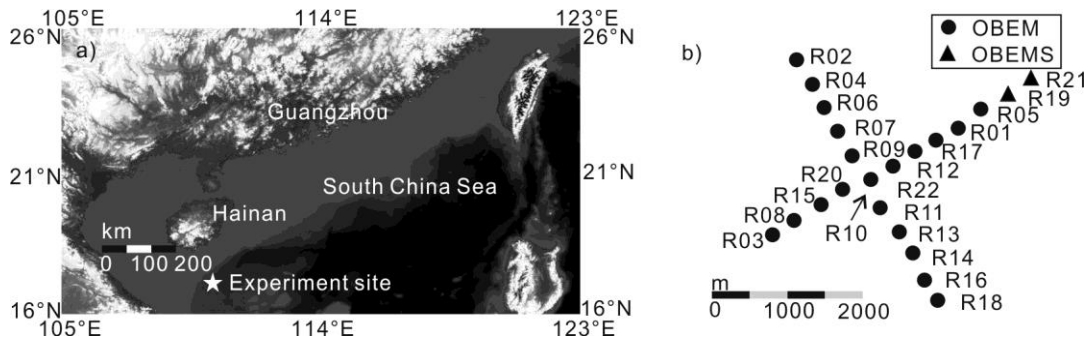
Fig. 5. Photograph of the offshore experiment area and site map with all receiver locations marked. The map was generated using the Global Mapper software package.

400
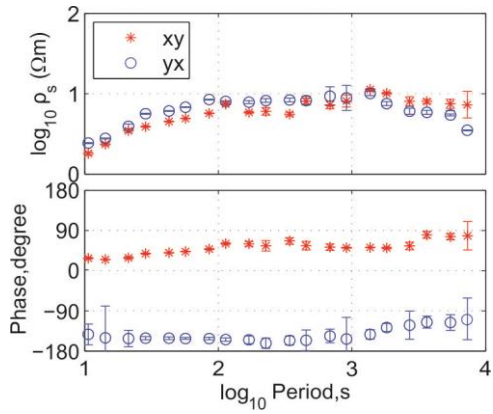
405   **Fig. 6. Apparent resistivity (top) and phase (bottom) curves calculated from the OBEMS E-field and B-field at site R19. The red star indicates the xy component and the blue circles indicate the yx component.**
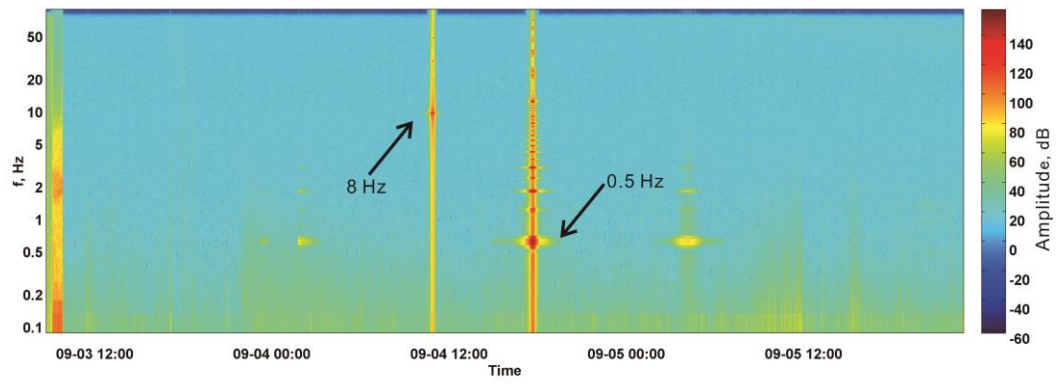
410 **Fig. 7. Short time Fourier transform results for the CSEM signal from the horizontal electrical field components.**
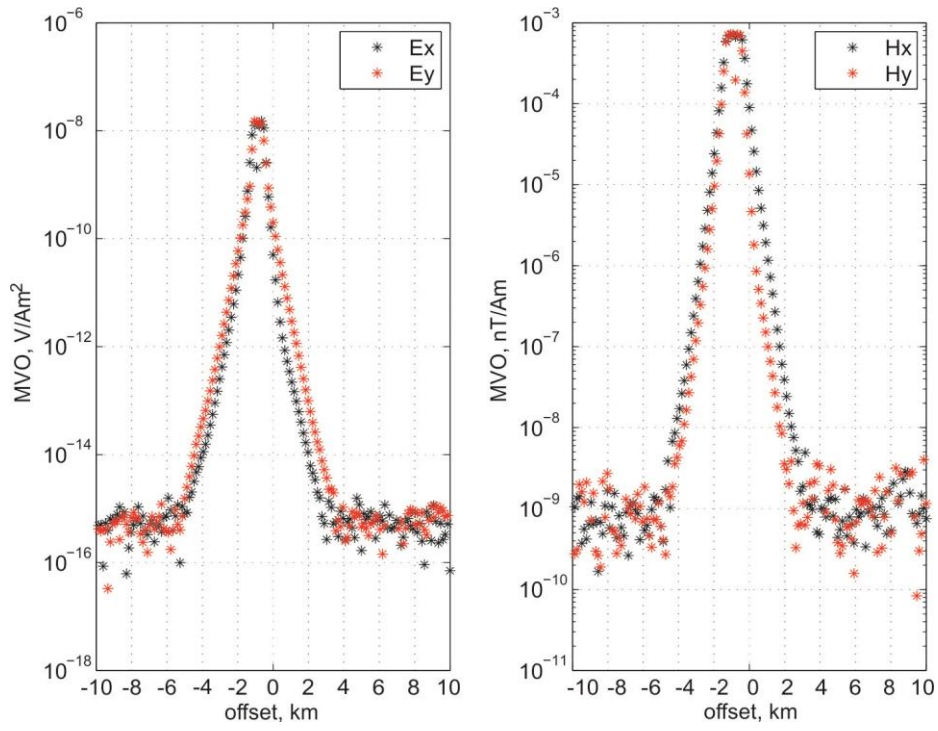
Fig. 8. Magnitude versus offset for the E and H components (site: R19, frequency: 8 Hz).

415
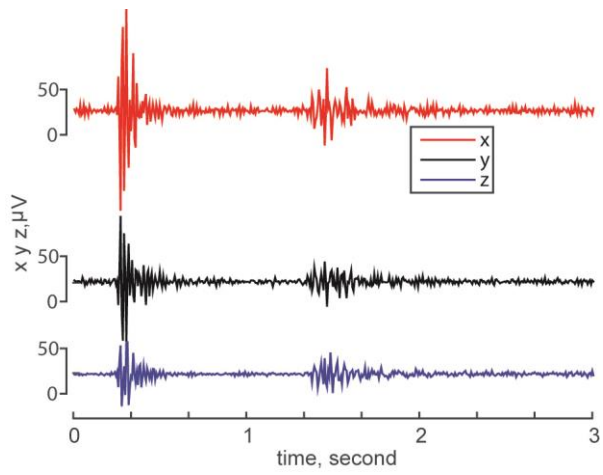
Fig. 9. Seismic data acquisition test results in real environmental conditions from the OBEMS at test site R21. (a) First horizontal component, (b) second horizontal component, and (c) vertical geophone component.

420
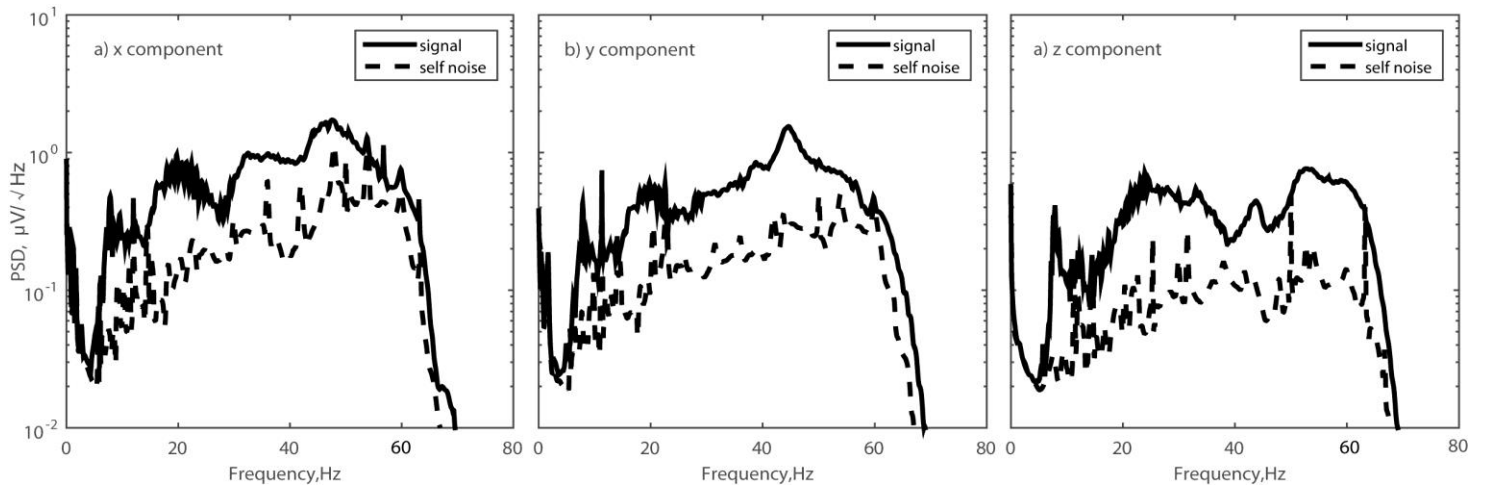
Fig. 10. Power spectral density (PSD) of the signal and self-noise in real environmental conditions from the OBEMS at test site R21. (a) First horizontal component, (b) second horizontal component, and (c) vertical geophone component.

425

Table 1. Technical specifications for the ocean bottom electromagnetic receiver and seismometer (OBEMS).

Channels	7 Ex\Ey, Geophone (x,y,z), Hx, Hy
Sensor Type	Electrode: Ag/AgCl
	Magnetic sensor: induction coil
	Geophone: Triaxial, Orthogonal, omnidirectional moving coil
Channel –3 dB band width @ fs = 2,400 Hz	E field: 0.01 Hz to 100 Hz
	Induction coil: 0.1–500 Hz
	Geophone: 8–300 Hz
Maximum battery lifetime	30 days
Memory	32 GB SD card (upgrade 128 GB)
Release mechanism	USBL motor drive release and burn wire release
Weight	114 kg in air (exclude anchor)
	–32 kg in water
Electrode dipole	12 m
Dynamic range	E field channel: 110 dB @, B field channel: 130 dB @ fs = 1,000 Hz
	Seismic channel: 130 dB @ fs = 1,000 Hz
Position in water	USBL responder
Sensitivity	Geophone: 78.5 V/m/s at 15 Hz
	Induction coil: 0.3 V/nT
Gain preamplifier	E field channel: 480 to 30720 step 2
	B filed channel: 0.4 to 25.6 step 2
	Geophone: 20 to 56 dB step 6 dB
Noise level	E field: 0.1 nV/m/rt (Hz) @ 1 Hz
	B field: 0.1 pT/rt(Hz) @ 1 Hz
Time drift error	Less than 2 ms/day
Maxim Work water depth	4,000 m
User interface	USB & WiFi (data transfer rate 3 MB/s)

430